High energy protons and neutrinos from γ-ray bursts

Eli Waxman

Weizmann Institute of Science, Rehovot 76100, Israel

(Received October 19, 2001)

A review is presented of the fireball model of γ-ray bursts (GRBs), and of the production in GRB fireballs of high energy protons and neutrinos. Constraints imposed on the model by recent afterglow observations, which support the association of GRB and ultra-high energy cosmic-ray (UHECR) sources, are discussed. Predictions of the model, which can be tested with planned large area UHECR detectors and with planned high energy neutrino telescopes, are reviewed.

KEYWORDS: gamma-rays: bursts—cosmic rays—acceleration of particles—elementary particles

§1. Introduction

The widely accepted interpretation of the phenomenology of γ-ray bursts (GRBs), bursts of 0.1 MeV–1 MeV photons lasting for a few seconds,[1] is that the observable effects are due to the dissipation of the kinetic energy of a relativistically expanding wind, a "fireball," whose primal cause is not yet known.[2] The recent detection of "afterglows," delayed low energy (X-ray to radio) emission of GRBs,[3] confirmed the cosmological origin of the bursts, through the redshift determination of several GRB host-galaxies, and confirmed standard model predictions of afterglows that result from the collision of an expanding fireball with its surrounding medium.[4]

The fireball model is described in §2. We do not discuss in this section the issue of GRB progenitors, i.e. the underlying sources producing the relativistic fireballs. At present, the two leading progenitor scenarios are collapses of massive stars,[5] and mergers of compact objects.[6] As explained in §2, the evolution of the fireball and the emission of γ-rays and afterglow radiation (on time scale of a day and longer) are largely independent of the nature of the progenitor. Thus, although present observations provide stringent constraints on the fireball model, the underlying progenitors remain unknown.[3,4,7]

In §3 we discuss the association of GRBs and ultra-high energy cosmic-rays (UHECRs).[8] We show that recent afterglow observations strengthen the evidence for GRB and UHECR association, which is based on two key points. First, the constraints imposed on fireball model parameters by recent observations imply that acceleration of protons is possible to energy higher than previously estimated, $\sim 10^{21}$ eV. Second, the inferred local ($z = 0$) GRB energy generation rate of γ-rays, $\sim 10^{44}$erg/Mpc^{3}yr, is remarkably similar to the local generation rate of UHECRs implied by cosmic-ray observations.

The GRB model for UHECR production makes unique predictions,[8,9] that may be tested with planned large area UHECR detectors.[10] These predictions are described in §4. In particular, a critical energy is predicted to exist, $10^{20}\text{eV} \leq \epsilon_c < 4 \times 10^{20}\text{eV}$, above which a few sources produce most of the UHECR flux, and the observed spectra of these sources is predicted to be narrow, $\Delta\epsilon/\epsilon \sim 1$: the bright sources at high energy should be absent in UHECRs of much lower energy, since particles take longer to arrive the lower their energy. If the sources predicted by this model are detected by planned large area UHECR detectors, this would not only confirm the GRB model for UHECR production, but will also provide constraints on the unknown structure and strength of the inter-galactic magnetic field.

We note, that the AGASA experiment has recently reported the presence of one triplet and 3 doublets of UHECR events above 4×10^{19}eV, with angular separations (within each group) $\leq 2.5°$, roughly consistent with the measurement error.[11] The probability that these multiplets are chance coincidences (as opposed to being produced by point sources) is $\sim 1\%$. This possible detection of point sources at the highest energies favors the bursting source model (see §4.1), although more data are needed to confirm it. Testing the predictions of the fireball model for UHECR production would require an exposure 10 times larger than that of present experiments. Such increase is expected to be provided by the HiRes and Auger detectors, and by the proposed Telescope Array detector.[10]

Predictions for the emission of high energy neutrinos from GRB fireballs are discussed in §5. Implications for planned high energy neutrino telescopes[12] (the ICECUBE extension of AMANDA, ANTARES, NESTOR) are discussed in detail in §5.4. It is shown that the predicted flux of $\geq 10^{14}$ eV neutrinos may be detectable by Cerenkov neutrino telescopes while the flux above 10^{19} eV may be detectable by large air-shower detectors.[13,14] Detection of the predicted neutrino signal will confirm the GRB fireball model for UHECR production and may allow to discriminate between different fireball progenitor scenarios. Moreover, a detection of even a handful of neutrino events correlated with GRBs will allow to test for neutrino properties, e.g. flavor oscillation and coupling to gravity, with accuracy many orders of magnitude better than currently possible.

§2. The fireball model

2.1 The underlying scenario

In the fireball model of GRBs, a compact source of linear scale $r_0 \sim 10^7$ cm produces a wind characterized by an average luminosity $L \sim 10^{52}\mathrm{erg\,s^{-1}}$ and mass loss rate $\dot{M} = L/\eta c^2$. At small radius, the wind bulk Lorentz factor, Γ, grows linearly with radius, $\Gamma \propto r$, until most of the wind energy is converted to kinetic energy and Γ saturates, $\Gamma \sim \eta \sim 300$, at $r \sim \eta r_0$. Variability of the source on time scale Δt, resulting in fluctuations in the wind bulk Lorentz factor Γ on similar time scale, then leads to internal shocks in the expanding fireball at a radius

$$r_i \approx 2\Gamma^2 c\Delta t. \tag{2.1}$$

If the Lorentz factor variability within the wind is significant, internal shocks reconvert a substantial part of the kinetic energy to internal energy. It is assumed that this energy is then radiated as γ-rays by synchrotron and inverse-Compton emission of shock-accelerated electrons.

In this model, the observed γ-ray variability time, $\sim r_i/\Gamma^2 c \approx \Delta t$, reflects the variability time of the underlying source, and the GRB duration, $T \sim 10$s, reflects the duration over which energy is emitted from the source. A large fraction of bursts detected by BATSE show variability on the shortest resolved time scale, ~ 10 ms,[15] and some show variability on shorter time scales, ~ 1 ms.[16] This sets the constraint on underlying source size, $r_0 < c\Delta t \sim 10^7$ cm. The wind must be expanding relativistically, with a Lorentz factor $\Gamma \sim 300$, in order that the fireball pair-production optical depth be small for observed high energy, ~ 100 MeV, GRB photons.[17]

2.2 The allowed range of Lorentz factors and baryon loading

The acceleration, $\Gamma \propto r$, of fireball plasma is driven by radiation pressure. Fireball protons are accelerated through their coupling to the electrons, which are coupled to fireball photons. We have assumed above, that photons and electrons are coupled throughout the acceleration phase. However, if the baryon loading is too low, radiation may decouple from fireball electrons already at $r < \eta r_0$. The fireball Thomson optical depth is given by the product of comoving expansion time, $r/\Gamma(r)c$, and the photon Thomson scattering rate, $n_e c\sigma_T$. The electron and proton comoving number densities are equal, $n_e = n_p$, and are determined by equating the r independent mass flux carried by the wind, $4\pi r^2 c\Gamma(r) n_p m_p$, to the mass loss rate from the underlying source, which is related to the rate L at which energy is emitted through $\dot{M} = L/(\eta c^2)$. Thus, during the acceleration phase, $\Gamma(r) = r/r_0$, the Thomson optical depth $\tau_T \propto r^{-3}$. τ_T drops below unity at a radius $r < r_f = \eta r_0$ if $\eta > \eta_*$, where

$$\eta_* = \left(\frac{\sigma_T L}{4\pi r_0 m_p c^3}\right)^{1/4} = 1.0\times 10^3 L_{52}^{1/4} r_{0,7}^{-1/4}. \tag{2.2}$$

Here $r_0 = 10^7 r_{0,7}$ cm.

If $\eta > \eta_*$ radiation decouples from the fireball plasma at $\Gamma = r/r_0 = \eta_*^{4/3}\eta^{-1/3}$. If $\eta \gg \eta_*$, then most of the radiation energy is not converted to kinetic energy prior to radiation decoupling, and most of the fireball energy escapes in the form of thermal radiation. Thus, the baryon load of fireball shells, and the corresponding final Lorentz factors, must be within the range $10^2 \le \Gamma \approx \eta \le \eta_* \approx 10^3$ in order to allow the production of the observed non-thermal γ-ray spectrum.

2.3 γ-ray emission

If the Lorentz factor variability within the wind is significant, internal shocks would reconvert a substantial part of the kinetic energy to internal energy. The internal energy may then be radiated as γ-rays by synchrotron and inverse-Compton emission of shock-accelerated electrons. The internal shocks are expected to be "mildly" relativistic in the fireball rest frame, i.e. characterized by Lorentz factor $\Gamma_i - 1 \sim$ a few. This is due to the fact that the allowed range of shell Lorentz factors is $\sim 10^2$ to $\sim 10^3$ (see §2.2), implying that the Lorentz factors associated with the relative velocities are not very large. Since internal shocks are mildly relativistic, we expect results related to particle acceleration in sub-relativistic shocks[18] to be valid for acceleration in internal shocks. In particular, electrons are expected to be accelerated to a power law energy distribution, $dn_e/d\gamma_e \propto \gamma_e^{-p}$ for $\gamma_e > \gamma_m$, with $p \simeq 2$.

The minimum Lorentz factor γ_m is determined by the following consideration. Protons are heated in internal shocks to random velocities (in the wind frame) $\gamma_p^R - 1 \approx \Gamma_i - 1 \approx 1$. If electrons carry a fraction ξ_e of the shock internal energy, then $\gamma_m \approx \xi_e(m_p/m_e)$. The characteristic frequency of synchrotron emission is determined by γ_m and by the strength of the magnetic field. Assuming that a fraction ξ_B of the internal energy is carried by the magnetic field, $4\pi r_i^2 c\Gamma^2 B^2/8\pi = \xi_B L_{\mathrm{int.}}$, the characteristic observed energy of synchrotron photons, $\epsilon_{\gamma b} = \Gamma\hbar\gamma_m^2 eB/m_e c$, is

$$\epsilon_{\gamma b} \approx 1\xi_B^{1/2}\xi_e^{3/2}\frac{L_{\gamma,52}^{1/2}}{\Gamma_{2.5}^2\Delta t_{-2}}\mathrm{MeV}. \tag{2.3}$$

In deriving Eq. (2.3) we have assumed that the wind luminosity carried by internal plasma energy, $L_{\mathrm{int.}}$, is related to the observed γ-ray luminosity through $L_{\mathrm{int.}} = L_\gamma/\xi_e$. This assumption is justified since the electron synchrotron cooling time is short compared to the wind expansion time (unless the equipartition fraction ξ_B is many orders of magnitude smaller than unity), and hence electrons lose all their energy radiatively. Fast electron cooling also results in a synchrotron spectrum $dn_\gamma/d\epsilon_\gamma \propto \epsilon_\gamma^{-1-p/2} = \epsilon_\gamma^{-2}$ at $\epsilon_\gamma > \epsilon_{\gamma b}$, consistent with observed GRB spectra.

At present, there is no theory that allows the determination of the values of the equipartition fractions ξ_e and ξ_B. Eq. (2.3) implies that fractions not far below unity are required to account for the observed γ-ray emission. We note, that build up of magnetic field to near equipartition by electro-magnetic instabilities is expected to be a generic characteristic of collisionless shocks,[18] and is inferred to occur in other systems, e.g. in supernova remnant shocks.[19]

The γ-ray break energy $\epsilon_{\gamma b}$ of most GRBs observed by BATSE detectors is in the range of 100 keV to 300 keV.[1] It may appear from Eq. (2.3) that the clustering of break energies in this narrow energy range requires fine tuning of fireball model parameters, which should naturally produce a much wider range of break energies. This is, however, not the case.[20] Consider the dependence of $\epsilon_{\gamma b}$ on Γ. For values of Γ smaller than $\approx 10^{2.5}$, most of the high energy photons in the power-law distribution produced by synchrotron emission, $dn_\gamma/d\epsilon_\gamma \propto \epsilon_\gamma^{-2}$, would be converted to pairs. This would lead to high optical depth due to Thomson scattering on $e^\pm$, and hence to strong suppression of the emitted flux.[20] As explained in §2.2, shell Lorentz factors can not exceed $\eta_* \simeq 10^3$, for which break energies in the X-ray range, $\epsilon_{\gamma b} \sim 10$ keV, may be obtained. The radiative flux would be strongly suppressed if the typical Γ of radiation emitting shells is close to η_*, since in this case the range of Lorentz factors of wind shells is narrow, which implies that only a small fraction of wind kinetic energy would be converted to internal energy which can be radiated from the fireball.

Thus, the clustering of break energies at ~ 1 MeV is naturally accounted for, provided that the variability time scale satisfies $\Delta t \leq 10^{-2}$ s, which implies an upper limit on the source size, since $\Delta t \geq r_0/c$. In addition, a natural consequence of the model is the existence of low luminosity bursts with low, 1 keV to 10 keV, break energies.[20] Such "X-ray bursts" may have recently been identified.[21]

2.4 Afterglow emission

As the fireball expands, it drives a relativistic shock (blast-wave) into the surrounding gas. At early time, $t \ll T$, the fireball is little affected by this external interaction. At late time, $t \gg T$, most of the fireball energy is transferred to the surrounding gas, and the flow approaches the Blandford-McKee self-similar flow.[22] The shock driven into the ambient medium continuously heats fresh gas, and accelerates relativistic electrons which produce through synchrotron emission the delayed radiation, "afterglow," observed on time scales of days to months. As the shock-wave decelerates, due to accumulation of ambient gas mass, the emission shifts with time to lower frequencies. For expansion into uniform density gas, the shock Lorentz factor decreases with time according to $\Gamma_{BM}(t) \propto t^{-3/8}$.

During the transition to self-similar expansion, which takes place on (observed) time scale comparable to T, reverse shocks propagate into the fireball ejecta and decelerate it. At this stage the shocked plasma expands with the self-similar Lorentz factor, which for expansion into uniform density gas is given by[23]

$$\Gamma_{BM}(t=T) \simeq 245 \left(\frac{E_{53}}{n_0}\right)^{1/8} T_1^{-3/8}, \tag{2.4}$$

while the unshocked fireball ejecta propagate with the original expansion Lorentz factor, $\Gamma = \eta > \Gamma_{BM}(t=T)$. Here, $E = 10^{53} E_{53}$ erg is the total fireball energy, $T = 10\,T_1$ s, and $n = 1\,n_0 \mathrm{cm}^{-3}$ is the ambient gas density. $n_0 = 1$ is typical to the interstellar medium. Similar to internal shocks, the reverse shocks are also expected to be mildly relativistic, since the ratio $\eta/\Gamma_{BM}(t=T)$ is not far from unity.

§3. UHECRs from GRB fireballs

3.1 Fermi acceleration in GRBs

In the fireball model, the observed radiation is produced, both during the GRB and the afterglow, by synchrotron emission of shock accelerated electrons. In the region where electrons are accelerated, protons are also expected to be shock accelerated. This is similar to what is thought to occur in supernovae remnant shocks, where synchrotron radiation of accelerated electrons is the likely source of non-thermal X-rays (recent ASCA observations[24] give evidence for acceleration of electrons in the remnant of SN1006 to 10^{14}eV), and where shock acceleration of protons is believed to produce cosmic rays with energy extending to $\sim 10^{15}$eV.[18] Thus, it is likely that protons, as well as electrons, are accelerated to high energy within GRB fireballs. Let us consider the constraints that should be satisfied by the fireball parameters in order to allow acceleration of protons to $\sim 10^{20}$ eV.

We consider proton Fermi acceleration in fireball internal shocks, which take place as the fireball expands over a range of radii, $r \sim \Gamma^2 r_0$ to $r \sim \Gamma^2 c T_{\rm GRB}$, and at the reverse shocks driven into fireball ejecta due to interaction with surrounding medium at $r \sim \Gamma^2 cT \sim \Gamma^2 c T_{\rm GRB}$ (see §2). Both internal and reverse shocks are, in the wind rest-frame, mildly relativistic, i.e. characterized by Lorentz factors $\Gamma_i - 1 \sim 1$. Moreover, since reverse shocks do not cause strong deceleration of fireball plasma, see §2.4, the expansion Lorentz factor $\Gamma_{BM}(t=T)$ of fireball plasma shocked by reverse shocks is similar to the fireball Lorentz factor Γ prior to interaction with the surrounding medium. Thus, plasma parameters, e.g. energy and number density, in the reverse shocks are similar to those obtained in internal shocks due to variability on time scale $\Delta t \sim T$. Results obtained below for internal shocks are therefore valid also for reverse shocks, provided Δt is replaced with T.

Since the shocks we are interested in are mildly relativistic, we expect results related to particle acceleration in sub-relativistic shocks[18] to be valid for our scenario. The predicted energy distribution of accelerated protons is therefore $dn_p/d\epsilon_p \propto \epsilon_p^{-2}$, similar to the predicted electron energy spectrum, which is consistent with the observed photon spectrum (see §2.3).

The most restrictive requirement, which rules out the possibility of accelerating particles to energy $\sim 10^{20}$ eV in most astrophysical objects, is that the particle Larmor radius R_L should be smaller than the system size.[25] In our scenario we must apply a more stringent requirement, namely that R_L should be smaller than the largest scale l over which the magnetic field fluctuates, since otherwise Fermi acceleration may not be efficient. We may estimate l as follows. The comoving time, i.e. the time measured in the wind rest frame, is $t = r/\Gamma c$. Thus, regions separated by a comoving distance larger than r/Γ are causally disconnected, and the wind properties fluctuate over comoving length scales up to $l \sim r/\Gamma$. We must therefore require $R_L < r/\Gamma$. A somewhat more stringent requirement is related to the wind expansion. Due to expansion the internal energy is decreasing and therefore available for proton acceleration (as well as for γ-ray production) only over a comoving time $t \sim r/\Gamma c$. The typical Fermi acceleration time is[18,25] $t_a = fR_L/c\beta^2$, where βc is the Alfvén velocity and $f \sim 1$. In our scenario $\beta \simeq 1$ leading to the requirement $fR_L < r/\Gamma$. This condition sets a lower limit to the required comoving magnetic field strength.[26–28] Using the relations $R_L = \epsilon_p'/eB = \epsilon_p/\Gamma eB$, where $\epsilon_p' = \epsilon_p/\Gamma$ is the proton energy measured in the fireball frame, and $4\pi r^2 c\Gamma^2 B^2/8\pi = \xi_B L_\gamma/\xi_e$, the constraint $fR_L < r/\Gamma$ may be written as,[26]

$$\xi_B/\xi_e > 0.02 f^2 \Gamma_{2.5}^2 \epsilon_{p,20}^2 L_{\gamma,52}^{-1}, \tag{3.1}$$

where $\epsilon_p = 10^{20}\epsilon_{p,20}$ eV is the accelerated proton energy. Note, that this constraint is independent of r, the internal collision radius.

The accelerated proton energy is also limited by energy loss due to synchrotron radiation and interaction with fireball photons. As discussed in §5, the dominant energy loss process is synchrotron cooling. The condition that the synchrotron loss time, $t_{sy} = (6\pi m_p^4 c^3/\sigma_T m_e^2)\epsilon_p^{-1}B^{-2}$, should be smaller than the acceleration time sets an upper limit to the magnetic field strength. Since the equipartition field decreases with radius, $B_{e.p.} \propto r^{-1}$, the upper limit on the magnetic field may be satisfied simultaneously with (3.1) provided that the internal collisions occur at large enough radius,[26]

$$r > 10^{12} f^2 \Gamma_{2.5}^{-2} \epsilon_{p,20}^3 \text{cm}. \tag{3.2}$$

Since collisions occur at radius $r \approx \Gamma^2 c\Delta t$, the condition (3.2) is equivalent to a lower limit on Γ

$$\Gamma > 130 f^{1/2} \epsilon_{p,20}^{3/4} \Delta t_{-2}^{-1/4}. \tag{3.3}$$

From Eqs. (3.1) and (3.3), we infer that a dissipative ultra-relativistic wind, with luminosity and variability time implied by GRB observations, satisfies the constraints necessary to allow the acceleration of protons to energy $> 10^{20}$ eV, provided that the wind bulk Lorentz factor is large enough, $\Gamma > 100$, and that the magnetic field is close to equipartition with electrons. The former constraint, $\Gamma > 100$, is remarkably similar to that inferred based on the γ-ray spectrum, and $\Gamma \sim 300$ is the "canonical" value assumed in the fireball model. The latter constraint, magnetic field close to equipartition, must be satisfied to account for both γ-ray emission (see §2.3) and afterglow observations.

It has recently been claimed[29] that the conditions at the external shock driven by the fireball into the ambient gas are not likely to allow proton acceleration to ultra-high energy. Regardless of the validity of this claim, it is irrelevant for the acceleration in internal shocks. Moreover, it is not at all clear that UHECRs can not be produced at the external shock, since the magnetic field may be amplified ahead of the shock by the streaming of high energy particles. Proton production in the external shock and its possible implications were discussed by Dermer.[30]

The determination of GRB redshifts implies that the characteristic GRB γ-ray luminosity and emitted energy, in the 0.05 to 2 MeV band, are $L_\gamma \sim 10^{52}$erg/s and $E_\gamma \sim 10^{53}$erg respectively, an order of magnitude higher than the values assumed prior to afterglow detection (here, and throughout the paper, we assume a flat universe, $\Omega = 0.3$, $\Lambda = 0.7$, and $H_0 = 65$ km/s Mpc). The increased GRB luminosity scale implies that the constraint (3.1) on the fireball magnetic field is less stringent than previously assumed.

We have assumed in the discussion so far that the fireball is spherically symmetric. However, since a jet-like fireball behaves as if it were a conical section of a spherical fireball as long as the jet opening angle is larger than Γ^{-1}, our results apply also for a jet-like fireball (we are interested only in processes that occur when the wind is ultra-relativistic, $\Gamma \sim 300$, prior to significant fireball deceleration). For a jet-like wind, L in our equations should be understood as the luminosity the fireball would have carried had it been spherically symmetric.

3.2 Energy generation rate

The observed GRB redshift distribution implies a typical GRB γ-ray energy of $E \approx 2 \times 10^{53}$ erg, and a GRB rate of $R_{\rm GRB} \sim 3/\text{Gpc}^3\text{yr}$ at $z \sim 1$. The present, $z = 0$, rate is less well constrained, since most observed GRBs originate at redshifts $1 \le z \le 2.5$.[3] Present data are consistent with both no evolution of GRB rate with redshift, and with strong evolution (following, e.g., star formation rate), in which $R_{\rm GRB}(z=1)/R_{\rm GRB}(z=0) \sim 10$. Detailed analyses, assuming $R_{\rm GRB}$ is proportional to star formation rate, lead to $R_{\rm GRB}(z=0) \sim 0.5/\text{Gpc}^3\text{yr}$.[3] The energy observed in γ-rays reflect the fireball energy in accelerated electrons. If accelerated electrons and protons carry similar energy (as indicated by afterglow observations[31]) then the GRB cosmic-ray production rate is

$$\epsilon_p^2 (d\dot{n}_p/d\epsilon_p)_{z=0} \approx 10^{44} \text{erg/Mpc}^3\text{yr}. \tag{3.4}$$

In Fig. 1 we compare the observed UHECR spectrum with that predicted by the GRB model (assuming GRB rate follows star formation rate). The generation rate (3.4) of high energy protons is remarkably similar to that required to account for the flux of $> 10^{19}$ eV cosmic-rays. The flux at lower energies is most likely dominated by heavy nuclei of Galactic origin,[32] as indicated by the flattening of the spectrum at $\approx 10^{19}$ eV and by the evidence for a change in composition at this energy.[35]

The suppression of model flux above $10^{19.7}$ eV is due to energy loss of high energy protons in interaction with the microwave background, i.e. to the "GZK cutoff."[36] The available data do not allow to determine the existence (or absence) of the "cutoff" with high confidence. The AGASA results show an excess (at a $\sim 2.5\sigma$ confidence level) of events compared to model predictions above 10^{20}eV. This excess is not confirmed, however, by the other experiments. Moreover, since the 10^{20}eV flux is dominated by sources at distances < 100 Mpc,

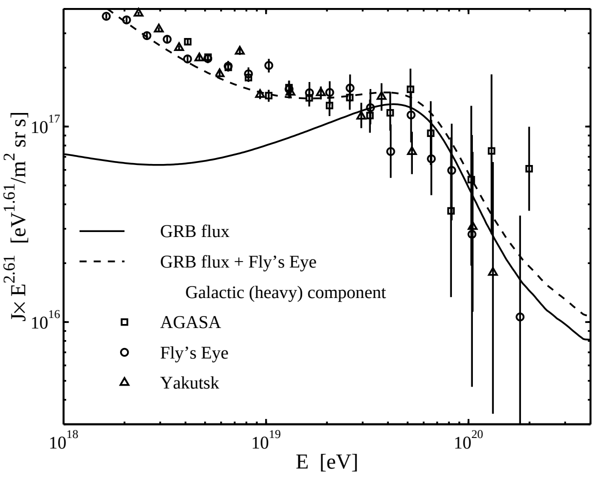

Fig. 1. The UHECR flux expected in a cosmological model, where high-energy protons are produced at a rate $(\epsilon_p^2 d\dot{n}_p/d\epsilon_p)_{z=0} = 0.8\times 10^{44}\mathrm{erg/Mpc^3yr}$ as predicted in the GRB model [Eq. (3.4)], solid line, compared to the Fly's Eye,[32)] Yakutsk[33)] and AGASA[34)] data. 1σ flux error bars are shown. The highest energy points are derived assuming the detected events represent a uniform flux over the energy range 10^{20} eV–3×10^{20} eV. The dashed line is the sum of the GRB model flux and the Fly's Eye fit (with normalization increased by 25%) to the Galactic heavy nuclei component,[32)] $J_G \propto E^{-3.5}$, which dominates below $\sim 10^{19}$ eV.

over which the distribution of known astrophysical systems (e.g. galaxies, clusters of galaxies) is inhomogeneous, significant deviations from model predictions presented in Fig. 1 for a uniform source distribution are expected at this energy.[37)] Clustering of cosmic-ray sources leads to a standard deviation, σ, in the expected number, N, of events above 10^{20} eV, given by[38)] $\sigma/N = 0.9(d_0/10\mathrm{Mpc})^{0.9}$, where d_0 is the unknown scale length of the source correlation function and $d_0 \sim 10$ Mpc for field galaxies.

The AGASA excess above 10^{20} eV has recently been used[39)] to argue that GRBs can not produce the observed cosmic-rays above 10^{20} eV. This claim was made without assessing the statistical significance of the excess, ignoring the Fly's Eye and Yakutsk data, and ignoring the effects of inhomogeneities, which are expected to be dominant at this energy range.

Thus, GRB fireballs would produce UHECR flux and spectrum consistent with that observed, provided the efficiency with which the wind kinetic energy is converted to γ-rays, and therefore to electron energy, is similar to the efficiency with which it is converted to proton energy, i.e. to UHECRs.[26)] There is, however, one additional point which requires consideration.[26)] The energy of the most energetic cosmic ray detected by the Fly's Eye experiment is in excess of 2×10^{20}eV, and that of the most energetic AGASA event is $\sim 2\times10^{20}$eV. On a cosmological scale, the distance traveled by such energetic particles is small: < 100Mpc (50Mpc) for the AGASA (Fly's Eye) event.[40)] Thus, the detection of these events over a $\sim$ 5yr period can be reconciled with the rate of nearby GRBs, $\sim$ 1 per 100 yr to $\sim$ 1 per 1000 yr out to 100Mpc, only if there is a large dispersion, $\geq$ 100yr, in the arrival time of protons produced in a single burst (This implies that if a direct correlation between high energy CR events and GRBs, as suggested by Milgrom & Usov,[28)] is observed on a $\sim$ 10yr time scale, it would be strong evidence *against* a cosmological GRB origin of UHECRs).

The required dispersion is likely to occur due to the combined effects of deflection by random magnetic fields and energy dispersion of the particles.[26)] Consider a proton of energy ϵ_p propagating through a magnetic field of strength B and correlation length λ. As it travels a distance λ, the proton is typically deflected by an angle $\alpha \sim \lambda/R_L$, where $R_L = \epsilon_p/eB$ is the Larmor radius. The typical deflection angle for propagation over a distance D is $\theta_s \approx (2D/9\lambda)^{1/2}\lambda/R_L$. This deflection results in a time delay, compared to propagation along a straight line,

$$\tau(\epsilon_p, D) \approx \theta_s^2 D/4c \approx 10^7 \epsilon_{p,20}^{-2} D_{100}^2 \lambda_{\mathrm{Mpc}} B_{-8}^2 \quad \mathrm{yr}, \quad (3.5)$$

where $D = 100D_{100}$Mpc, $\lambda = 1\lambda_{\mathrm{Mpc}}$ Mpc and $B = 10^{-8}B_{-8}$ G. Here, we have chosen numerical values corresponding to the current upper bound on the intergalactic magnetic field,[41)] $B\lambda^{1/2} \leq 10^{-8}$G Mpc$^{1/2}$. The upper bound on the (systematic increase with redshift of the) Faraday rotation measure of distant, $z \leq 2.5$, radio sources, $RM < 5\mathrm{rad/m^2}$, implies an upper bound $B \leq 10^{-11}(h/0.75)(\Omega_b h^2)^{-1}$ G on an inter-galactic field coherent over cosmological scales.[41)] Here, h is the Hubble constant in units of 100km/s Mpc and Ω_b is the baryon density in units of the closure density. For a magnetic field coherent on scales $\sim \lambda$, this implies $B\lambda^{1/2} \leq 10^{-8}(h/0.65)^{1/2}(\Omega_b h^2/0.02)^{-1}$G Mpc$^{1/2}$.

The random energy loss UHECRs suffer as they propagate, owing to the production of pions, implies that at any distance from the observer there is some finite spread in the energies of UHECRs that are observed with a given fixed energy. For protons with energies $> 10^{20}$eV the fractional RMS energy spread is of order unity over propagation distances in the range[40)] $10-100$Mpc. Since the time delay is sensitive to the particle energy, this implies that the spread in arrival time of UHECRs with given observed energy is comparable to the average time delay at that energy $\tau(\epsilon_p, D)$ (This result has been confirmed by numerical calculations[42)]). Thus, the required time spread, $\tau > 100$ yr, is consistent with the upper bound, $\tau < 10^7$ yr, implied by the present upper bound to the inter-galactic magnetic field.

§4. GRB model predictions for UHECR experiments

4.1 The Number and Spectra of Bright Sources

The initial proton energy, necessary to have an observed energy ϵ_p, increases with source distance due to propagation energy losses. The rapid increase of the initial energy after it exceeds, due to electron-positron production, the threshold for pion production effectively introduces a cutoff distance, $D_c(\epsilon_p)$, beyond which sources do not contribute to the flux above ϵ_p. The function

$D_c(\epsilon_p)$ is shown in Fig. 3 (adapted from[9]). Since $D_c(\epsilon_p)$ is a decreasing function of ϵ_p, for a given number density of sources there is a critical energy ϵ_c, above which only one source (on average) contributes to the flux. In the GRB model ϵ_c depends on the product of the burst rate R_{GRB} and the time delay. The number of sources contributing, on average, to the flux at energy ϵ_p is[9]

$$N(\epsilon_p) = \frac{4\pi}{5} R_{GRB} D_c(\epsilon_p)^3 \tau\left[\epsilon_p, D_c(\epsilon_p)\right] \quad , \qquad (4.1)$$

and the average intensity resulting from all sources is

$$J(\epsilon_p) = \frac{1}{4\pi} R_{GRB} \frac{dn_p}{d\epsilon_p} D_c(\epsilon_p) \quad , \qquad (4.2)$$

where $dn_p/d\epsilon_p$ is the number per unit energy of protons produced on average by a single burst (this is the formal definition of $D_c(\epsilon_p)$). The critical energy ϵ_c is given by

$$\frac{4\pi}{5} R_{GRB} D_c(\epsilon_c)^3 \tau\left[\epsilon_c, D_c(\epsilon_c)\right] = 1 \quad . \qquad (4.3)$$

ϵ_c, the energy beyond which a single source contributes on average to the flux, depends on the unknown properties of the inter-galactic magnetic field, $\tau \propto B^2\lambda$. However, the rapid decrease of $D_c(\epsilon_p)$ with energy near 10^{20}eV implies that ϵ_c is only weakly dependent on the value of $B^2\lambda$, as shown in Fig. 2. In The GRB

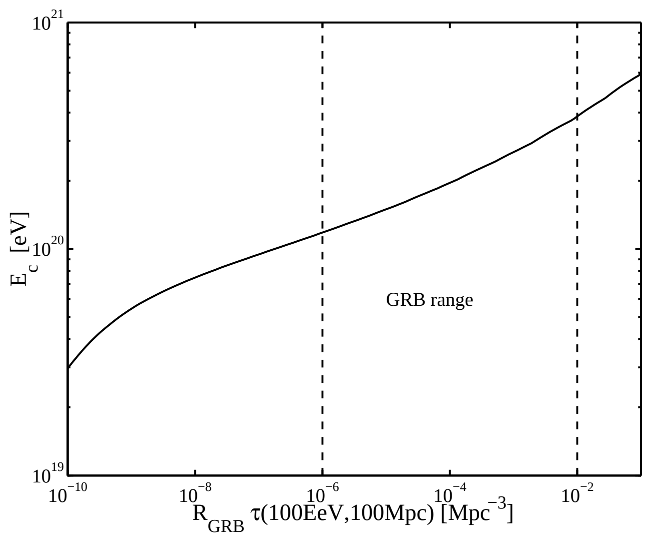

Fig. 2. ϵ_c, the energy beyond which a single GRB contributes on average to the UHECR flux, as a function of the product of GRB rate, $R_{\rm GRB} \approx 1/{\rm Gpc}^3$, and the time delay of a 10^{20} eV proton originating at 100 Mpc distance. The time delay depends on the unknown inter-galactic field, $\tau \propto B^2\lambda$. Dashed lines show the allowed range of $B^2\lambda$: The lower limit is set by the requirement that at least a few GRB sources be present at $D < 100$ Mpc, and the upper limit by the Faraday rotation bound[41] $B\lambda^{1/2} \le 10^{-8}{\rm G~Mpc}^{1/2}$, see Eq. (3.5) and the discussion the follows it.

model, the product $R_{GRB}\tau(D = 100{\rm Mpc}, \epsilon_p = 10^{20}{\rm eV})$ is approximately limited to the range 10^{-6} Mpc^{-3} to 10^{-2} Mpc^{-3} [The lower limit is set by the requirement that at least a few GRB sources be present at $D <$ 100 Mpc, and the upper limit by the Faraday rotation bound[41] $B\lambda^{1/2} \le 10^{-8}$G Mpc$^{1/2}$ see Eq. (3.5), and $R_{GRB} \le 1/$ Gpc^{3}yr]. The corresponding range of values of ϵ_c is $10^{20}{\rm eV} \le \epsilon_c < 4 \times 10^{20}$eV.

Fig. 3 presents the flux obtained in one realization of a Monte-Carlo simulation described by Miralda-Escudé & Waxman[9] of the total number of UHECRs received from GRBs at some fixed time. For each realization the posi-

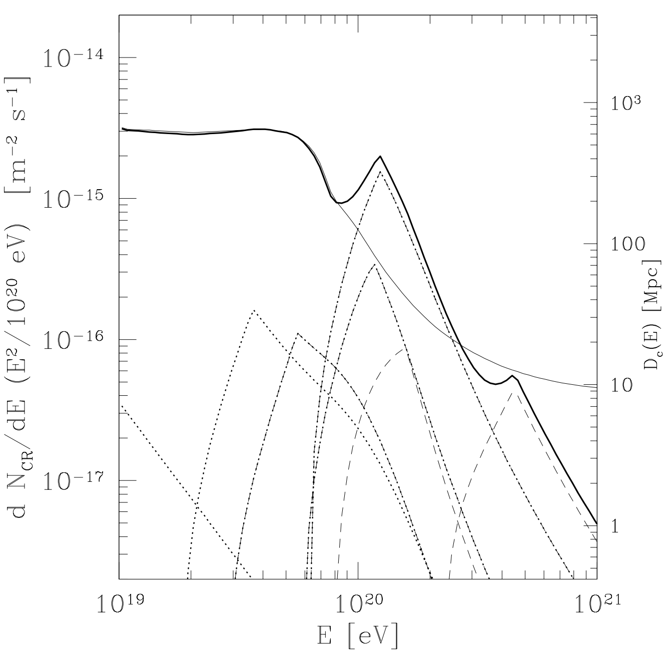

Fig. 3. Results of a Monte-Carlo realization of the bursting sources model, with $\epsilon_c = 1.4 \times 10^{20}$ eV: Thick solid line- overall spectrum in the realization; Thin solid line- average spectrum, this curve also gives $D_c(\epsilon_p)$; Dotted lines- spectra of brightest sources at different energies.

tions (distances from Earth) and times at which cosmological GRBs occurred were randomly drawn, assuming an intrinsic proton generation spectrum $dn_p/d\epsilon_p \propto \epsilon_p^{-2}$, and $\epsilon_c = 1.4 \times 10^{20}$eV. Most of the realizations gave an overall spectrum similar to that obtained in the realization of Fig. 3 when the brightest source of this realization (dominating at 10^{20}eV) is not included. At $\epsilon_p < \epsilon_c$, the number of sources contributing to the flux is very large, and the overall UHECR flux received at any given time is near the average (the average flux is that obtained when the UHECR emissivity is spatially uniform and time independent). At $\epsilon_p > \epsilon_c$, the flux will generally be much lower than the average, because there will be no burst within a distance $D_c(\epsilon_p)$ having taken place sufficiently recently. There is, however, a significant probability to observe one source with a flux higher than the average. A source similar to the brightest one in Fig. 3 appears $\sim 5\%$ of the time.

At any fixed time a given burst is observed in UHECRs only over a narrow range of energy, because if a burst is currently observed at some energy ϵ_p then UHECRs of much lower energy from this burst have not yet arrived, while higher energy UHECRs reached us mostly in the past. As mentioned above, for energies above the pion production threshold, $\epsilon_p \sim 5 \times 10^{19}$eV, the dispersion in arrival times of UHECRs with fixed observed energy is comparable to the average delay at that energy. This implies that the spectral width $\Delta\epsilon_p$ of t he source at a given time is of order the average observed energy, $\Delta\epsilon_p \sim \epsilon_p$. Thus, bursting UHECR sources should have narrowly peaked energy spectra, and the brightest sources should be different at different energies. For steady state sources, on the other hand, the brightest source at high energies should also be the brightest one at low energies, its fractional contribution to the overall flux decreasing to low energy only as $D_c(\epsilon_p)^{-1}$. A detailed numerical analysis of the time dependent energy spectrum of bursting sources is given in refs.[43]

4.2 Spectra of Sources at $\epsilon_p < 4 \times 10^{19}$eV

The detection of UHECRs above 10^{20}eV imply that the brightest sources must lie at distances smaller than 100Mpc. UHECRs with $\epsilon_p \leq 4\times10^{19}$eV from such bright sources will suffer energy loss only by pair production, because at $\epsilon_p < 5 \times 10^{19}$ eV the mean-free-path for pion production interaction (in which the fractional energy loss is $\sim$ 10%) is larger than 1Gpc. Furthermore, the energy loss due to pair production over 100Mpc propagation is only $\sim$ 5%.

In the case where the typical displacement of the UHECRs due to deflections by inter-galactic magnetic fields is much smaller than the correlation length, $\lambda \gg D\theta_s(D, \epsilon_p) \simeq D(D/\lambda)^{1/2}\lambda/R_L$, all the UHECRs that arrive at the observer are essentially deflected by the same magnetic field structures, and the absence of random energy loss during propagation implies that all rays with a fixed observed energy would reach the observer with exactly the same direction and time delay. At a fixed time, therefore, the source would appear mono-energetic and point-like. In reality, energy loss due to pair production results in a finite but small spectral and angular width, $\Delta\epsilon_p/\epsilon_p \sim \delta\theta/\theta_s \leq 1\%$.[9]

In the case where the typical displacement of the UHECRs is much larger than the correlation length, $\lambda \ll D\theta_s(D, \epsilon_p)$, the deflection of different UHECRs arriving at the observer are essentially independent. Even in the absence of any energy loss there are many paths from the source to the observer for UHECRs of fixed energy ϵ_p that are emitted from the source at an angle $\theta \leq \theta_s$ relative to the source-observer line of sight. Along each of the paths, UHECRs are deflected by independent magnetic field structures. Thus, the source angular size would be of order θ_s and the spread in arrival times would be comparable to the characteristic delay τ, leading to $\Delta\epsilon_p/\epsilon_p \sim 1$ even when there are no random energy losses. The observed spectral shape of a nearby ($D <$ 100Mpc) bursting source of UHECRs at $\epsilon_p < 4 \times 10^{19}$eV was derived for the case $\lambda \ll D\theta_s(D, \epsilon_p)$ in by Waxman and Miralda-Escudé,[9] and is given by

$$\frac{dN}{d\epsilon_p} \propto \sum_{n=1}^{\infty}(-1)^{n+1}\, n^2\, \exp\left[-\frac{2n^2\pi^2\epsilon^2}{\epsilon_0^2(t,D)}\right] \quad , \qquad (4.4)$$

where $\epsilon_0(t, D) = De(2B^2\lambda/3ct)^{1/2}$. For this spectrum, the ratio of the RMS UHECR energy spread to the average energy is 30%

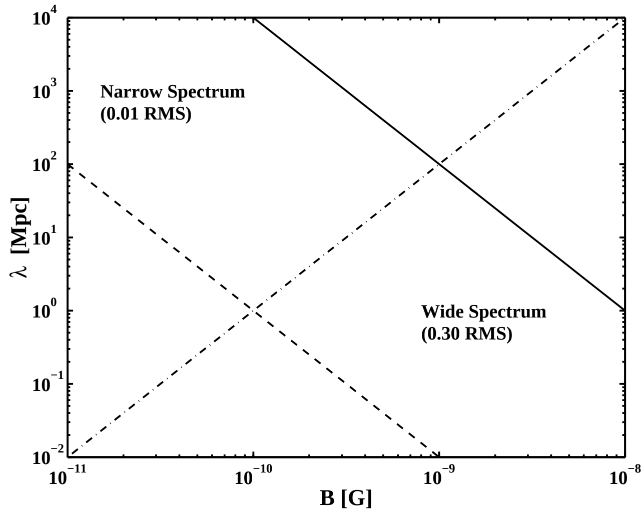

Fig. 4. The line $\theta_s D = \lambda$ for a source at 30Mpc distance observed at energy $\epsilon_p \simeq 10^{19}$eV (dot-dash line), shown with the Faraday rotation upper limit $B\lambda^{1/2} \leq 10^{-8}$G Mpc$^{1/2}$ (solid line), and with the lower limit $B\lambda^{1/2} \geq 10^{-10}$G Mpc$^{1/2}$ required in the GRB model [see Eq. (3.5)].

Fig. 4 shows the line $\theta_s D = \lambda$ in the $B - \lambda$ plane, for a source at a distance D = 30Mpc observed at energy $\epsilon_p \simeq 10^{19}$eV. Since the $\theta_s D = \lambda$ line divides the allowed region in the plane at $\lambda \sim$ 1Mpc, measuring the spectral width of bright sources would allow to determine if the field correlation length is much larger, much smaller, or comparable to 1Mpc.

§5. GRB Neutrinos

5.1 Internal shock (GRB) neutrinos

5.1.1 Neutrinos at energies $\sim 10^{14}$ *eV.*

Protons accelerated in the fireball to high energy lose energy through photo-meson interaction with fireball photons. The decay of charged pions produced in this interaction, $\pi^+ \to \mu^+ + \nu_\mu \to e^+ + \nu_e + \overline{\nu}_\mu + \nu_\mu$, results in the production of high energy neutrinos. The key relation is between the observed photon energy, ϵ_γ, and the accelerated proton's energy, ϵ_p, at the threshold of the Δ-resonance. In the observer frame,

$$\epsilon_\gamma\, \epsilon_p = 0.2\,\mathrm{GeV}^2\,\Gamma^2\ . \qquad (5.1)$$

For $\Gamma \approx 300$ and $\epsilon_\gamma = 1$ MeV, we see that characteristic proton energies $\sim 10^{16}$ eV are required to produce pions. Since neutrinos produced by pion decay typically carry 5% of the proton energy (see below), production of $\sim 10^{14}$ eV neutrinos is expected.[44]

The fractional energy loss rate of a proton with energy $\epsilon_p' = \epsilon_p/\Gamma$ measured in the wind rest frame due to pion production is

$$t_\pi^{-1}(\epsilon_p') \equiv -\frac{1}{\epsilon_p'}\frac{d\epsilon_p'}{dt} = \frac{1}{2\gamma_p^2}c\int_{\epsilon_0}^{\infty} d\epsilon\, \sigma_\pi(\epsilon)\xi(\epsilon)\epsilon$$

$$\times \int_{\epsilon/2\Gamma_p}^{\infty} dx\, x^{-2} \frac{dn_\gamma}{d\epsilon_\gamma}(\epsilon_\gamma = x)\,, \qquad (5.2)$$

where $\gamma_p = \epsilon'_p/m_p c^2$, $\sigma_\pi(\epsilon)$ is the cross section for pion production for a photon with energy ϵ in the proton rest frame, $\xi(\epsilon)$ is the average fraction of energy lost to the pion, $\epsilon_0 = 0.15$GeV is the threshold energy, and $dn_\gamma/d\epsilon_\gamma$ is the photon density per unit photon energy in the wind rest frame. In deriving Eq. (5.2) we have assumed that the photon distribution in the wind rest frame is isotropic. The GRB photon spectrum is well fitted in the BATSE detector range, 20 keV to 2 MeV, by a combination of two power-laws,[1)] $dn_\gamma/d\epsilon_\gamma \propto \epsilon_\gamma^{-\beta}$, with $\beta \simeq 1$ at $\epsilon_\gamma < \epsilon_{\gamma b}$, $\beta \simeq 2$ at $\epsilon_\gamma > \epsilon_{\gamma b}$ and $\epsilon_{\gamma b} \sim 1$MeV. Thus, the second integral in (5.2) may be approximated by

$$\int_{\epsilon}^{\infty} \mathrm{d}x\, x^{-2} \frac{dn_\gamma}{d\epsilon_\gamma}(\epsilon_\gamma = x) \simeq \frac{1}{1+\beta} \frac{U_\gamma}{2\epsilon'^3_{\gamma b}} \left(\frac{\epsilon}{\epsilon'_{\gamma b}}\right)^{-(1+\beta)}, \qquad (5.3)$$

where U_γ is the photon energy density (in the range corresponding to the observed BATSE range) in the wind rest-frame, $\beta = 1$ for $\epsilon < \epsilon'_{\gamma b}$ and $\beta = 2$ for $\epsilon > \epsilon'_{\gamma b}$. $\epsilon'_{\gamma b}$ is the break energy measured in the wind frame, $\epsilon'_{\gamma b} = \epsilon_{\gamma b}/\Gamma$. The main contribution to the first integral in (5.2) is from photon energies $\epsilon \sim \epsilon_{\rm peak} = 0.3$GeV, where the cross section peaks due to the Δ resonance. Approximating the integral by the contribution from the resonance we obtain

$$t_\pi^{-1}(\epsilon'_p) \simeq \frac{U_\gamma}{2\epsilon'_{\gamma b}} c\sigma_{\rm peak}\xi_{\rm peak} \frac{\Delta\epsilon}{\epsilon_{\rm peak}} \min(1, 2\gamma_p\epsilon'_{\gamma b}/\epsilon_{\rm peak})\,. \qquad (5.4)$$

Here, $\sigma_{\rm peak} \simeq 5 \times 10^{-28}{\rm cm}^2$ and $\xi_{\rm peak} \simeq 0.2$ are the values of σ and ξ at $\epsilon = \epsilon_{\rm peak}$, and $\Delta\epsilon \simeq 0.2$GeV is the peak width.

The energy loss of protons due to pion production is small during the acceleration process. Once accelerated, the time available for proton energy loss by pion production is comparable to the wind expansion time as measured in the wind rest frame, $t_{\rm co} \sim r/\Gamma c$. Thus, the fraction of energy lost by protons to pions is $f_\pi \simeq r/\Gamma c t_\pi$. The energy density in the BATSE range, U_γ, is related to the luminosity L_γ by $L_\gamma = 4\pi r^2\Gamma^2 c U_\gamma$. Using this relation in (5.4), and $r = 2\Gamma^2 c\Delta t$, f_π is given by[44)]

$$f_\pi(\epsilon_p) \approx 0.1 \frac{L_{\gamma,52}}{\epsilon_{\gamma b,{\rm MeV}}\Gamma_{2.5}^4 \Delta t_{-2}} \times \begin{cases} 1, & \text{if } \epsilon_p > \epsilon_{pb}; \\ \epsilon_p/\epsilon_{pb}, & \text{otherwise.} \end{cases} \qquad (5.5)$$

The proton break energy is

$$\epsilon_{pb} \approx 10^{16}\Gamma_{2.5}^2(\epsilon_{\gamma b,{\rm MeV}})^{-1}\,{\rm eV}\,. \qquad (5.6)$$

The value of f_π, Eq. (5.5), is strongly dependent on Γ. It has recently been pointed out[45)] that if the Lorentz factor Γ varies significantly between bursts, with burst to burst variations $\Delta\Gamma/\Gamma \sim 1$, then the resulting neutrino flux will be dominated by a few neutrino bright bursts, and may significantly exceed the flux implied by Eq. (5.5), derived for typical burst parameters. This may strongly enhance the detectability of GRB neutrinos by planned neutrino telescopes.[46)] However, as explained in §2.2, the Lorentz factors of fireballs producing observed GRBs can not differ significantly from $\Gamma \simeq 250$: Lower Lorentz factors lead to optically thick fireballs, while higher Lorentz factors lead to low luminosity X-ray bursts (which may have already been identified). A detailed analysis, using Monte-Carlo simulations of the internal shock model,[47)] confirms that for fireball parameter range consistent with observed GRB characteristics, f_π at $\epsilon_p > \epsilon_{pb}$ is limited to the range of $\sim 10\%$ to 30%.

Thus, for parameters typical of a GRB producing wind, a significant fraction of the energy of protons accelerated to energies larger than the break energy, $\sim 10^{16}$eV, would be lost to pion production. Roughly half of the energy lost by protons goes into π^0 's and the other half to π^+ 's. Neutrinos are produced by the decay of π^+'s, $\pi^+ \to \mu^+ + \nu_\mu \to e^+ + \nu_e + \overline{\nu}_\mu + \nu_\mu$ [the large optical depth for high energy γ's from π^0 decay would not allow these photons to escape the wind]. The mean pion energy is 20% of the energy of the proton producing the pion. This energy is roughly evenly distributed between the π^+ decay products. Thus, approximately half the energy lost by protons of energy ϵ_p is converted to neutrinos with energy $\sim 0.05\epsilon_p$. Eq. (5.5) then implies that the spectrum of neutrinos above $\epsilon_{\nu b} = 0.05\epsilon_{pb}$ follows the proton spectrum, and is harder (by one power of the energy) at lower energy.

If GRBs are the sources of UHECRS, then using Eq. (3.4) the expected GRB neutrino flux is[44)]

$$\epsilon_\nu^2\Phi_{\nu_\mu} \approx \epsilon_\nu^2\Phi_{\bar\nu_\mu} \approx \epsilon_\nu^2\Phi_{\nu_e} \approx \frac{c}{4\pi}\frac{f_\pi}{8}\epsilon_p^2(d\dot n_p/d\epsilon_p)t_H \approx 10^{-9}\frac{f_\pi(\epsilon_{pb})}{0.2}\min\left(1, \frac{\epsilon_\nu}{\epsilon_{\nu b}}\right)\frac{\rm GeV}{{\rm cm^2 s\, sr}}, \qquad (5.7)$$

where $t_H \approx 10^{10}$ yr is the Hubble time. The factor of 1/8 is due to the fact that charged pions and neutral pions are produced with roughly equal probabilities (and each neutrino carries $\sim 1/4$ of the pion energy).

The GRB neutrino flux can also be estimated directly from the observed gamma-ray fluence. The BATSE detectors measure the GRB fluence F_γ over two decades of photon energy, ~ 0.02MeV to ~ 2MeV, corresponding to a decade of radiating electron energy (the electron synchrotron frequency is proportional to the square of the electron Lorentz factor). If electrons carry a fraction ξ_e of the energy carried by protons, then the muon neutrino fluence of a single burst is $\epsilon_\nu^2 dN_\nu/d\epsilon_\nu \approx 0.25(f_\pi/\xi_e)F_\gamma/\ln(10)$. The average neutrino flux per unit time and solid angle is obtained by multiplying the single burst fluence with the GRB rate per solid angle, $\approx 10^3$ bursts per year over 4π sr. Using the average burst fluence $F_\gamma = 10^{-5}{\rm erg/cm}^2$, we obtain a muon neutrino flux $\epsilon_\nu^2\Phi_\nu \approx 3\times 10^{-9}(f_\pi/\xi_e){\rm GeV/cm^2 s\,sr}$. Thus, the neutrino flux estimated directly from the gamma-ray fluence agrees with the estimate (5.7) based on the cosmic-ray production rate.

5.1.2 Neutrinos at energy $> 10^{16}$ eV.

The neutrino spectrum (5.7) is modified at high energy, where neutrinos are produced by the decay of muons and pions whose life time $\tau_{\mu,\pi}$ exceeds the characteristic time for energy loss due to adiabatic expansion and synchrotron emission.[44,48)] The synchrotron loss time is determined by the energy density of the magnetic field in the wind rest frame. For the characteristic parameters of a GRB wind, the muon energy for which the adiabatic energy loss time equals the muon life time, ϵ_μ^a, is comparable to the energy ϵ_μ^s at which the life time equals the synchrotron loss time, τ_μ^s. For pions, $\epsilon_\pi^a > \epsilon_\pi^s$. This, and the fact that the adiabatic loss time is independent of energy and the synchrotron loss time is inversely proportional to energy, imply that synchrotron losses are the dominant effect suppressing the flux at high energy. The energy above which synchrotron losses suppress the neutrino flux is

$$\frac{\epsilon^s_{\nu_\mu(\bar\nu_\mu,\nu_e)}}{\epsilon_{\nu b}} \approx \left(\frac{\xi_B}{\xi_e} L_{\gamma,52}\right)^{-1/2} \Gamma^2_{2.5}\Delta t_{-2}\epsilon_{\gamma b,\mathrm{MeV}} \times \begin{cases} 10, & \text{for } \bar\nu_\mu,\, \nu_e; \\ 100, & \text{for } \nu_\mu\ . \end{cases} \quad (5.8)$$

The efficiency of neutrino production in internal collisions decreases with Δt, $f_\pi \propto \Delta t^{-1}$ [see Eq. (5.5)], since the radiation energy density is lower at larger collision radii. However, at larger radii synchrotron losses cut off the spectrum at higher energy, $\epsilon^s(\Delta t) \propto \Delta t$ [see Eq. (5.8)]. Collisions at large radii therefore result in extension of the neutrino spectrum of Eq. (5.7) to higher energy, beyond the cutoff energy Eq. (5.8),

$$\epsilon_\nu^2 \Phi_\nu \propto \epsilon_\nu^{-1}, \quad \epsilon_\nu > \epsilon_\nu^s. \quad (5.9)$$

5.2 Afterglow neutrinos, $\sim 10^{18}$ eV

During the transition to self-similarity, protons and electrons are accelerated to high energy in the reverse shocks. High energy protons may interact with the 10 eV–1 keV photons radiated by the electrons, to produce through pion decay a burst of duration $\sim T$ of ultra-high energy, 10^{17}–10^{19} eV, neutrinos[23] as indicated by Eq. (5.1).

While afterglows have been detected in several cases, reverse shock emission has only been identified for GRB 990123.[49] Both the detections and the non-detections are consistent with shocks occurring with typical model parameters,[50] suggesting that reverse shock emission may be common. The predicted neutrino emission depends, however, upon parameters of the surrounding medium that can only be estimated once more observations of the prompt optical afterglow emission are available.

If the density of gas surrounding the fireball is $n \sim 1\mathrm{cm}^{-3}$, a value typical to the inter-stellar medium and consistent with GRB 990123 observations, then the synchrotron emission of reverse shock electrons is expected to peak in the X-ray band, $\epsilon_\gamma \approx 1$ keV, with luminosity[23] $L_X \approx 2 \times 10^{50}$erg/s. Using these parameters in Eq. (5.5), replacing Δt with $T \approx 10$ s and recalling that $\Gamma = 250$ at the reverse shock stage [see Eq.(2.4)], we find $f_\pi \approx 0.01$ for protons of energy 10^{19} eV. Thus, the expected neutrino fluence for a typical burst, $E \approx 10^{53}$ erg at $z \sim 1$, is[23]

$$\epsilon_\nu^2 \Phi_{\nu_x} \approx 10^{-4.5} \left(\frac{\epsilon_\nu}{10^{17}\mathrm{eV}}\right)^\alpha \frac{\mathrm{GeV}}{\mathrm{cm}^2}, \quad (5.10)$$

where $\alpha = 1/2$ for $\epsilon_\nu > 10^{17}$eV and $\alpha = 1$ for $\epsilon_\nu < 10^{17}$eV. Here too, ν_x stands for ν_μ, $\bar\nu_\mu$ or ν_e. The value of α, $\alpha = 1/2$ for $\epsilon_\nu > 10^{17}$eV, corresponding to photomeson interactions with low energy photons, differs from the value $\alpha = 0$ in the case of internal shocks discussed in §5.1, since the low energy photon spectrum is different in the two cases: $dN_\gamma/d\epsilon_\gamma \propto \epsilon_\gamma^{-\beta}$ with $\beta = 1$ for internal shocks, and $\beta = 3/2$ for reverse shocks.

Some GRBs may result from the collapse of a massive star in which case the fireball is expected to expand into a pre-existing wind. For typical wind parameters, the transition to self-similar behavior takes place at a radius where the wind density is $n \approx 10^4\mathrm{cm}^{-3} \gg 1\mathrm{cm}^{-3}$. The higher density implies a lower Lorenz factor of the expanding plasma during the transition stage [see Eq. (2.4)], and hence a larger fraction of proton energy lost to pion production. Protons of energy $\epsilon_p \geq 10^{18}$ eV lose all their energy to pion production in this case, and a typical GRB at $z \sim 1$ is expected to produce a neutrino fluence[23,51]

$$\epsilon_\nu^2 \Phi_{\nu_x} \approx 10^{-2.5} \left(\frac{\epsilon_\nu}{10^{17}\mathrm{eV}}\right)^\alpha \frac{\mathrm{GeV}}{\mathrm{cm}^2}, \quad (5.11)$$

where $\alpha = 0$ for $\epsilon_\nu > 10^{17}$eV and $\alpha = 1$ for $\epsilon_\nu < 10^{17}$eV.

The neutrino flux is expected to be strongly suppressed at energy $> 10^{19}$ eV, since protons are not expected to be accelerated to energy $\gg 10^{20}$ eV.

5.3 Inelastic p-n collisions

The acceleration, $\Gamma \propto r$, of fireball plasma emitted from the source of radius r_0 (see §2.1) is driven by radiation pressure. Fireball protons are accelerated through their coupling to the electrons, which are coupled to fireball photons. Fireball neutrons, which are expected to exist in most progenitor scenarios, are coupled to protons by nuclear scattering as long as the comoving p-n scattering time is shorter than the comoving wind expansion time $r/\Gamma c = r_0/c$. As the fireball plasma expands and accelerates, the proton density decreases, $n_p \propto r^{-2}\Gamma^{-1}$, and neutrons may become decoupled. For $\eta > \eta_{pn}$, where

$$\eta_{pn} \approx 400 L_{52}^{1/4} r_{0,7}^{-1/4}, \quad (5.12)$$

neutrons decouple from the accelerating plasma prior to saturation, $\Gamma = \eta$, at $\Gamma = \eta_{pn}^{4/3}\eta^{-1/3}$.[52,53] In this case, relativistic relative velocities between protons and neutrons arise, which lead to pion production through inelastic nuclear collisions. Since decoupling occurs at a radius where the collision time is similar to wind expansion time, each n leads on average to one pair of $\nu\bar\nu$. The typical comoving neutrino energy, ~ 50 MeV, implies an observed energy ~ 10 GeV. A typical burst, $E = 10^{53}$ erg at $z = 1$, with significant neutron to proton ratio and $\eta > 400$ will therefore produce a fluence $F(\nu_e + \bar\nu_e) \sim 0.5F(\nu_\mu + \bar\nu_\mu) \sim 10^{-4}\mathrm{cm}^{-2}$ of ~ 10 GeV neutrinos.

Relativistic relative p-n velocities, leading to neutrino production through inelastic collisions, may also result from diffusion of neutrons [54] between regions of the fireball wind with large difference in Γ. If, for example, plasma expanding with very high Lorentz factor, $\Gamma > 100$, is confined to a narrow jet surrounded by a slower, $\Gamma\sim 10$ wind, internal collisions within the slower wind can heat neutrons to relativistic temperature, leading to significant diffusion of neutrons from the slower wind into the faster jet. Such process may operate for winds with $\eta<400$ as well as for $\eta>400$, and may lead, for certain (reasonable) wind parameter values, to ~ 10 GeV neutrino flux similar to that due to *p*-*n* decoupling in a $\eta>400$ wind.

5.4 Implications

The high energy neutrinos predicted in the dissipative wind model of GRBs may be observed by detecting the Cerenkov light emitted by high energy muons produced by neutrino interactions below a detector on the surface of the Earth.[55] The probability $P_{\nu\mu}$ that a neutrino would produce a high energy muon in the detector is approximately given by the ratio of the high energy muon range to the neutrino mean free path.[55] For the neutrinos produced in internal shocks, $\epsilon_\nu\sim 10^{14}$ eV, $P_{\nu\mu}\simeq 1.3\times 10^{-6}(\epsilon_\nu/1\mathrm{TeV})$. Using (5.7), the expected flux of neutrino induced muons is

$$J_\mu\approx 10\frac{f_\pi(\epsilon_{pb})}{0.2}\mathrm{km}^{-2}\mathrm{yr}^{-1}\,. \qquad (5.13)$$

The rate is almost independent of $\epsilon_{\nu b}$, due to the increase of $P_{\nu\mu}$ with energy. The rate (5.13) is comparable to the background expected due to atmospheric neutrinos.[55] However, neutrino bursts should be easily detected above the background, since the neutrinos would be correlated, both in time and angle, with the GRB γ-rays. A km^2 neutrino detector should detect each year ~ 10 neutrinos correlated with GRBs. Note, that at the high energies considered, knowledge of burst direction and time will allow to discriminate the neutrino signal from the background by looking not only for upward moving neutrino induced muons, but also by looking for down-going muons.

The predicted flux of $\sim 10^{17}$ eV neutrinos, produced by photo-meson interactions during the onset of fireball interaction with its surrounding medium, Eqs. (5.10,5.11), may be more difficult to detect. For the energy range of afterglow neutrinos, the probability $P_{\nu\mu}$ that a neutrino would produce a high energy muon with the currently required long path within the detector is[55,56] $P_{\nu\mu}\approx 3\times 10^{-3}(\epsilon_\nu/10^{17}\mathrm{eV})^{1/2}$. This implies, using (5.10) and a GRB rate of $10^3\mathrm{yr}^{-1}$, an expected detection rate of muon neutrinos of $\sim 0.06/\mathrm{km}^2\mathrm{yr}$ (over 2π sr), assuming fireballs explode in and expand into typical inter-stellar medium gas. If, on the other hand, most GRB progenitors are massive stars and fireballs expand into a pre-existing stellar wind, Eq. (5.11) implies a detection of several muon induced neutrinos per year in a 1km^3 detector. We note, that GRB neutrino detection rates may be significantly higher than derived based on the above simple arguments, because the knowledge of neutrino direction and arrival time may relax the requirement for long muon path within the detector.

Air-showers could be used to detect ultra-high energy neutrinos. The neutrino acceptance of the planned Auger detector, $\sim 10^4\mathrm{km}^3\mathrm{sr}$,[13] seems too low. The effective area of proposed space detectors[14] may exceed $\sim 10^6\mathrm{km}^2$ at $\epsilon_\nu>2\times 10^{19}$ eV, detecting several tens of GRB correlated events per year, provided that the neutrino flux extends to $\epsilon_\nu>2\times 10^{19}$ eV. Since, however, the GRB neutrino flux is not expected to extend well above $\epsilon_\nu\sim 10^{19}$ eV, and since the acceptance of space detectors decrease rapidly below $\sim 10^{19}$ eV, the detection rate of space detectors would depend sensitively on their low energy threshold.

Detection of high energy neutrinos will test the shock acceleration mechanism and the suggestion that GRBs are the sources of ultra-high energy protons, since $\geq 10^{14}$ eV ($\geq 10^{18}$ eV) neutrino production requires protons of energy $\geq 10^{16}$ eV ($\geq 10^{19}$ eV). The dependence of $\sim 10^{17}$ eV neutrino flux on fireball environment imply that the detection of high energy neutrinos will also provide constraints on GRB progenitors.

Inelastic *p*-*n* collisions may produce ~ 10 GeV neutrinos with a fluence of $\sim 10^{-4}\mathrm{cm}^{-2}$ per burst, due to either *p*-*n* decoupling in a wind with high neutron fraction and high, >400, Lorentz factor,[52,53] or to neutron diffusion in a wind with, e.g., strong deviation from spherical symmetry.[54] The predicted number of events in a 1km^3 neutrino telescope is $\sim 10\mathrm{yr}^{-1}$. Such events may be detectable in a suitably densely spaced detector. Detection of ~ 10 GeV neutrinos will constrain the fireball neutron fraction, and hence the GRB progenitor.

Detection of neutrinos from GRBs could be used to test the simultaneity of neutrino and photon arrival to an accuracy of ~ 1 s (~ 1 ms for short bursts), checking the assumption of special relativity that photons and neutrinos have the same limiting speed. These observations would also test the weak equivalence principle, according to which photons and neutrinos should suffer the same time delay as they pass through a gravitational potential. With 1 s accuracy, a burst at 100 Mpc would reveal a fractional difference in limiting speed of 10^{-16}, and a fractional difference in gravitational time delay of order 10^{-6} (considering the Galactic potential alone). Previous applications of these ideas to supernova 1987A,[57] where simultaneity could be checked only to an accuracy of order several hours, yielded much weaker upper limits: of order 10^{-8} and 10^{-2} for fractional differences in the limiting speed and time delay respectively.

The model discussed above predicts the production of high energy muon and electron neutrinos. However, if the atmospheric neutrino anomaly has the explanation it is usually given,[58] oscillation to ν_τ's with mass ~ 0.1 eV, then one should detect equal numbers of ν_μ's and ν_τ's. Up-going τ's, rather than μ's, would be a distinctive signature of such oscillations. Since ν_τ's are not expected to be produced in the fireball, looking for τ's would be an “appearance experiment.” To allow flavor change, the difference in squared neutrino masses, Δm^2, should exceed a minimum value proportional to the ratio of source distance and neutrino energy.[57] A burst at 100 Mpc producing 10^{14}eV neutrinos can test for $\Delta m^2\geq 10^{-16}\mathrm{eV}^2$, 5 orders of magnitude more sensitive than solar neutrinos.

Acknowledgments.

This work was supported in part by grants from the Israel-US BSF (BSF-9800343), MINERVA, and AEC

(AEC-38/99). EW is the Incumbent of the Beracha foundation career development chair.

---

1) For review see: Fishman, G. J. & Meegan, C. A., ARA&A **33**, 415 (1995).
2) For review see: Mészáros, P., Science, **291**, 79 (2001).
3) For review see: Kulkarni, S. R. *et al.*, To appear in Proc. of the 5th Huntsville Gamma-Ray Burst Symposium (astro-ph/0002168).
4) For review see: Mészáros, P., A&AS **138**, 533 (1999).
5) Woosley, S., Astrophys. J. **405**, 273 (1993); Paczyński, B., Astrophys. J. **494**, L45 (1998).
6) Paczyński, B., Astrophys. J. **308**, L43 (1986); Goodman, J., Astrophys. J. **308**, L47 (1986).
7) Livio, M. & Waxman, E., Astrophys. J. **538**, 187 (2000).
8) For review see: Waxman, E., Nucl. Phys. B (Proc. Suppl.) **87**, 345 (2000).
9) Miralda-Escudé, J. & Waxman, E., Astrophys. J. **462**, L59 (1996); Waxman, E. & Miralda-Escudé, J., Astrophys. J. **472**, L89 (1996).
10) For review see: Nagano, M. & Watson, A. A., Rev. Mod. Phys. **72**, 689 (2000).
11) Takeda, M. *et al.*, Ap. J. **522**, 225 (1999).
12) For review see: Halzen, F., in Proc. 17th International Workshop on Weak Interactions and Neutrinos (Cape Town, South Africa, January 1999) (astro-ph/9904216).
13) Capelle, K. S., Cronin, J. W., Parente, G., & Zas, E. Astropar. Phys. **8**, 321 (1998).
14) J. Linsley, Proc. 19th Intl. Cosmic-Ray conference, **3**, 438 (1985); Y. Takahashi, Proc. 24th Intl. Cosmic-Ray conference, **3**, 595 (1995).
15) Woods, E. & Loeb, A., Astrophys. J. **453**, 583 (1995).
16) Bhat, P. N., *et al.*, Nature **359**, 217 (1992).
17) Krolik, J. H. & Pier, E. A., Astrophys. J. **373**, 277 (1991).
18) For review see: Blandford, R., & Eichler, D., Phys. Rep. **154**, 1 (1987).
19) Helfand, D. J. & Becker, R. H., Ap. J., **314**, 203 (1987); Cargill, P. J. & Papadopoulos K., Ap. J., **329**, L29 (1988).
20) e.g.: Guetta, D., Spada M., & Waxman, E., to appear in Astrophys. J. (astro-ph/0011170).
21) Kippen, R. M., to appear in Proc. Second Rome Workshop: Gamma-Ray Bursts in the Aferglow Era (Rome, 2000) (astro-ph/0201277).
22) Blandford, R. D., & Mckee, C. F., Phys. Fluids **19**, 1130 (1976).
23) Waxman, E., & Bahcall, J. N., Astrophys. J. **541**, 707 (2000).
24) Koyama, K. *et al.*, Nature **378**, 255 (1995).
25) Hillas, A. M., ARA&A **22**, 425 (1984).
26) Waxman, E., Phys. Rev. Lett. **75**, 386 (1995).
27) Vietri, M., Ap. J. **453**, 883 (1995);
28) Milgrom, M. & Usov, V., Ap. J. **449**, L37 (1995).
29) Gallant, Y. A., & Achterberg, A., MNRAS **305**, L6 (1999).
30) Dermer, C. D., submitted to Ap. J. (astro-ph/0005440).
31) Freedman, D. L., & Waxman, E., Ap. J. **547**, 922 (2001).
32) Bird, D. J., *et al.*, Ap. J. **424**, 491 (1994).
33) Efimov, N. N. *et al.*, in *Proceedings of the International Symposium on Astrophysical Aspects of the Most Energetic Cosmic-Rays*, ed. M. Nagano and F. Takahara (World Scientific, Singapore, 1991), p. 20.
34) Takeda, M. *et al.*, Phys. Rev. Lett. **81**, 1163 (1998).
35) Dawson, B. R., Meyhandan, R., Simpson, K.M., Astropart. Phys. **9**, 331 (1998).
36) Greisen, K., Phys. Rev. Lett. **16**, 748 (1966); Zatsepin, G. T., & Kuzmin, V. A., JETP lett., **4**, 78 (1966).
37) Waxman, E., Ap. J. **452**, L1 (1995).
38) Bahcall, J. N., & Waxman, E., Ap. J. **542**, 542 (2000).
39) Stecker, F. W., Astropar. Phys. **14**, 207 (2000).
40) Aharonian, F. A., & Cronin, J. W., Phys. Rev. D **50**, 1892 (1994).
41) Kronberg, P. P., Rep. Prog. Phys. **57**, 325 (1994); Kronberg, P. P., Reinhardt, M. & Simard-Normandin, M., A&A **61**, 771 (1977).
42) Waxman, E., & Coppi, P., Ap. J. **464**, L75 (1996).
43) Lemoine, M., Sigl, G., Olinto, A. V. & Schramm, D. N., Ap. J. **486**, L115 (1997); Sigl, G., Lemoine, M. & Olinto, A. V., Phys. Rev. **D56**, 4470 (1997).
44) Waxman, E., & Bahcall, J. N., Phys. Rev. Lett. **78**, 2292 (1997); Phys. Rev. **D59**, 023002 (1999).
45) Halzen, F. & Hooper, D. W., Ap. J. **527**, L93 (1999).
46) Alvarez-Muniz, J., Halzen, F., & Hooper, D. W., Phys. Rev. **D62**, 093015 (2000).
47) Guetta, D., Spada M., & Waxman, E., to appear in Astrophys. J. (astro-ph/0102487).
48) Rachen, J. P., & Mészáros, P., Phys. Rev. D **58**, 123005 (1998).
49) Akerlof, C. W. *et al.*, Nature, **398**, 400 (1999).
50) Sari, R. & Piran, T., Ap. J. **517**, L109 (1999); Mészáros, P. & Rees, M., MNRAS **306**, L39 (1999).
51) Dai, Z. G., & Lu, T., submitted to Ap. J. (astro-ph/0002430).
52) Derishev, E. V., Kocharovsky, V. V., & Kocharovsky, Vl. V, Ap. J. **521**, 640 (1999).
53) Bahcall, J. N., & Mészáros, Phys. Rev. Lett., 85, 1362 (2000).
54) Mészáros, P., & Rees, M., Ap. J. **541**, L5 (2000).
55) For review see: Gaisser, T. K., Halzen, F., & Stanev, T., Phys. Rep. **258**, 173 (1995).
56) Gandhi, R., Quigg, C., Reno, M., & Sarcevic, I., Phys. Rev. **D58**, 093009 (1998).
57) For review see: J. N. Bahcall, *Neutrino Astrophysics*, Cambridge University Press (NY 1989), pp. 438–460.
58) Y. Fukuda *et al.*, Phys. Lett. **B335**, 237 (1994); D. Casper *et al.*, Phys. Rev. Lett. **66**, 2561 (1991); G. L. Fogli, and E. Lisi, Phys. Rev. **D52**, 2775 (1995).